Magnetocaloric effect in the intermetallic compounds $R\mathrm{Co}_2$ (R=Dy,Ho,Er)

N. A. de Oliveira,[1] P. J. von Ranke,[1] M. V. Tovar Costa,[1] and A. Troper[1,2]
[1]*Universidade do Estado de Rio de Janeiro, Rua São Francisco Xavier 524, Rio de Janeiro 20550-013, RJ, Brazil*
[2]*Centro Brasileiro de Pesquisas Físicas, Rua Dr. Xavier Sigaud 150, Rio de Janeiro 22290-180, RJ, Brazil*
(Received 13 December 2001; revised manuscript received 2 May 2002; published 4 September 2002)

In this paper we study the magnetocaloric effect in the rare-earth cobalt intermetallic compounds $R\mathrm{Co}_2$ (R=Dy, Ho, Er). We use a theoretical model, in which the localized spins of the rare-earth ions are immersed into an effective subsystem of the itinerant electrons. In the calculation of the magnetic entropy, we consider both the localized spins and the itinerant electrons contributions. The calculated curves of the adiabatic temperature change and of the isothermal magnetic entropy change with magnetic field for these intermetallic compounds show a jump around the magnetic ordering temperature, in good agreement with the experimental data.

DOI: 10.1103/PhysRevB.66.094402 PACS number(s): 75.30.Sg, 75.10.Dg, 75.20.En

I. INTRODUCTION

The magnetocaloric effect, the property of some magnetic materials to heat up or cool down when they are submitted to a varying magnetic field in an adiabatic process, has practical importance in the technological application of magnetic refrigeration.[1–6] Although the magnetocaloric effect is well known since the beginning of the last century, no real high-temperature applications have been made until very recently. The magnetocaloric effect is intrinsic to all magnetic materials and is measured both by the adiabatic temperature change $\Delta T_{ad}(T,h^{ext})$ and by the isothermal magnetic entropy change $\Delta S_{mag}(T,h^{ext})$ by an application or removal of an external magnetic field. Therefore these two characteristic quantities of the magnetocaloric effect depend on the temperature and on the magnetic-field variation.

The magnetocaloric effect has been investigated in perovskites,[7–9] magnetic molecular clusters,[10,11]and in rare-earth intermetallic compounds.[12–29]In recent years there has been increasing interest in the search for new magnetic materials with large magnetocaloric potentials. For instance, a giant magnetocaloric effect have been observed in the compounds $Gd_5Ge_2Si_2$,[2]$MnFeP_{0.45}As_{0.55}$,[30]and in high-spin molecular magnets.[10]Despite the large amount of experimental data on the magnetocaloric effect, there are only a few theoretical explanations for them.[10,13–17]As far as the rare-earth intermetallic compounds are concerned, some interesting experimental results have been reported for a wide range of temperature. For instance, we can mention the existence of a second peak in the magnetocaloric curves at low temperature;[28]the anomalous magnetocaloric effect,[13]where the increasing applied magnetic field makes the magnetic entropy to increase at low temperature; the tablelike effect,[12]where the peak in the isothermal magnetic entropy change remains constant along a small range of temperature; and the giant magnetocaloric effect,[2]where a large peak occurs in the magnetocaloric curves.

The theoretical models most used in the literature to study the magnetocaloric effect in rare-earth intermetallic compounds,[13–17]take mainly into account, in the calculation of the magnetic entropy, the contribution arising from the localized spins of the rare earth ions. These localized models including the crystalline electrical field have succeeded in explaining the experimental data of the magnetocaloric effect in the rare earth intermetallic compounds involving nonmagnetic atoms such as RNi_2, RAl_2, and RNi_5 among others.[13,17,21]In the framework of the localized models, the anomalous magnetocaloric effect observed in $PrNi_5$ is explained based on the crossing of the split $4f$ energy levels, due to the crystalline electrical field, with increasing magnetic field. However, the above-mentioned models fail to explain the magnetocaloric effect in the intermetallic compounds $R\mathrm{Co}_2$(R=Dy, Ho, Er). This is because these compounds exhibit special magnetic properties, namely: (i) a magnetic moment as large as 1.0 μ_B induced at the Co atoms; (ii) a first-order magnetic phase transition that is directly associated with the metamagnetism at the Co sites. These findings indicate that the $3d$ itinerant electrons play an important role in the magnetic and the thermodynamic properties of these intermetallic compounds. Thus, in the theoretical description of the magnetocaloric effect in the intermetallic compounds $R\mathrm{Co}_2$, we should consider both the localized spins and the itinerant electrons.

Based on the above considerations, in this work we theoretically study the magnetocaloric effect in the intermetallic compounds $R\mathrm{Co}_2$(R=Dy, Ho, Er). The understanding of the role of the $4f$ localized spins and the $3d$ itinerant electrons in the establishment of the magnetic order can give us a good insight in the physical mechanism that governs the magnetocaloric effect in these compounds for all range of temperatures. In order to carry out the calculations, we use a model Hamiltonian in which the $4f$ localized spins of the rare-earth ions are immersed into an effective subsystem of interacting $3d$ itinerant electrons. We also include the effect of the crystalline electrical field on the $4f$ spins of the rare-earth ions. For the sake of simplicity we use the Hartree-Fock approximation to treat the Coulomb interaction between the itinerant electrons and the molecular-field approximation to deal with the exchange interaction between $4f$ localized spins. The calculated curves of the adiabatic temperature change ($\Delta T_{ad}\times T$) and of the isothermal magnetic entropy change ($\Delta S_{mag}\times T$) for these intermetallic compounds show a jump around the magnetic ordering temperature, in good agreement with experimental data. The

plan of this paper is as follows. In Sec. II we present our model, whereas Sec. III is devoted to show our numerical calculations and discussions

II. THE MODEL

In order to describe the intermetallic compound $R\mathrm{Co}_2$ we begin with a model Hamiltonian in which the localized spins of the rare-earth ions are coupled to an effective subsystem of itinerant electrons.[31]

$$H = H^d + H^f + H^{df} + H^{CF}, \tag{1}$$

where

$$H^d = \sum_{i\sigma} \varepsilon_{0\sigma} d^+_{i\sigma} d_{i\sigma} + \sum_{il\sigma} T_{il\sigma} d^+_{i\sigma} d_{l\sigma} + U \sum_i n_{i\uparrow} n_{i\downarrow} - g_e \mu_B \sum_i s^d_i h^{ext}, \tag{2}$$

$$H^f = -J_0 \sum_{il} J^f_i . J^f_l - g_i \mu_B \sum_i J^f_i h^{ext}, \tag{3}$$

$$H^{df} = -J_{df} \sum_i J^f_i s^d_i, \tag{4}$$

$$H^{CF} = W\left[x \frac{O^0_4 + 5O^4_4}{F_4} + (1-|x|)\frac{(O^0_6 - 21O^4_6)}{F_6}\right]. \tag{5}$$

The Hamiltonian H^d describes a subsystem of itinerant electrons where the term $T_{il\sigma}$ represents the electron hopping energy between two different sites, U is the Coulomb interaction parameter between itinerant electrons, and h^{ext} represents the external magnetic field applied along the easy magnetization direction. The Hamiltonian H^f describes the subsystem of localized spins where J^f is the total angular momentum of the rare-earth ions and J_0 is the effective exchange interaction parameter between $4f$ localized spins. The Hamiltonian H^{df} gives the coupling between the localized spins and the itinerant electrons, where s^d_i is the spin of itinerant electrons and J_{df} is an effective exchange coupling parameter. Finally, H^{CF} is the crystalline electrical field Hamiltonian for the cubic symmetry,[32] where W is an energy scale and x gives the relative importance of the fourth- and sixth-order terms. O^n_m are the Stevens'operators; F_4 and F_6 are numerical factors common to all matrix elements.[33] The parameters g_i and g_e are the Landè factor of the rare-earth ions and the itinerant electrons, respectively. Using the Hartree-Fock approximation to treat the Coulomb interaction between the itinerant electrons and the molecular-field approximation to deal with the interaction between the localized spins, the Hamiltonian (1) can be written as

$$H^{eff}_d = \sum_i \left[\varepsilon_0 + U\langle n_{-\sigma}\rangle - \frac{1}{2}\sigma(J_{df}\langle J^f\rangle + g_e \mu_B h^{ext})\right] d^+_{i\sigma} d_{i\sigma} + \sum_{il} T_{il\sigma} d^+_{i\sigma} d_{l\sigma}, \tag{6}$$

$$H^{eff}_f = -\sum_i (J_0\langle J^f\rangle + J_{df}\langle s^d\rangle + g_i \mu_B h^{ext}) J^f_i + H^{CF}. \tag{7}$$

Now the Hamiltonian H^{eff}_d describes a subsystem of itinerant electrons under the action of the effective magnetic field generated by the $4f$ localized spins. The effective Hamiltonian H^{eff}_f describes a subsystem of $4f$ localized spins under the action of the crystalline electric field and coupled to the itinerant electrons. The problem defined by the coupled Hamiltonians H^{eff}_d and H^{eff}_f should be solved in a self-consistent way. The temperature dependence of the magnetization associated with the localized spins subsystem is given by $M^R = g_i \mu_B \langle J^f\rangle$, where $\langle J^f\rangle$ is the average of the total angular momentum of the rare-earth ions. On the other hand, the magnetic moment of the effective subsystem of the itinerant electrons is given by $M^d = n_\uparrow - n_\downarrow$, where n_σ ($\sigma = \uparrow$ or $\downarrow$) is the electron occupation number given by

$$n_\sigma = \int_{-\infty}^{\mu} \rho_\sigma(\varepsilon) f(\varepsilon) d\varepsilon, \tag{8}$$

where $\rho_\sigma(\varepsilon)$ is a spin-dependent density of states, $f(\varepsilon)$ is the Fermi distribution function, and μ is the chemical potential. Using the Green-function techniques we get the density of states $\rho_\sigma(\varepsilon)$ as

$$\rho_\sigma(\varepsilon) = -\frac{1}{\pi}\mathrm{Im}\int \frac{\rho_0(\omega) d\omega}{z - \varepsilon_{0\sigma}}, \tag{9}$$

where $z = \varepsilon + i0$, $\varepsilon_{0\sigma} = \varepsilon_0 + U\langle n_{-\sigma}\rangle - 0.5\sigma(J_{df}\langle J^f\rangle + g_e \mu_B h^{ext})$, and $\rho_0(\omega)$ is a standard paramagnetic model for $3d$ density of states. So the total magnetization of the intermetallic compound is given by the summation of the contribution of the itinerant electrons (M^d) and the localized spins (M^R) subsystems.

The magnetic entropy associated with the subsystem of localized spins is given by the relation[15–17]

$$S_{loc}(T, h^{ext}) = R\left[\ln \sum_i e^{-\beta E_i} + \frac{1}{kT}\frac{\sum_i E_i e^{-\beta E_i}}{\sum_i e^{-\beta E_i}}\right], \tag{10}$$

where E_i are the energy eigenvalues of the effective Hamiltonian (H^{eff}_f), R is the universal gas constant, and $\beta = 1/kT$, where k being the Boltzmann's constant. The free energy of the subsystem of itinerant electrons is given by[18,19]

$$F = -\frac{1}{\beta}\sum_\sigma \int_{a_\sigma}^{b_\sigma} \ln(1 + e^{-\beta(\varepsilon - \mu)})\rho_\sigma(\varepsilon) d\varepsilon, \tag{11}$$

where a_σ and b_σ are the bottom and the top of the spin-polarized density of states. The electronic magnetic entropy obtained by the thermodynamic relation $S_{el} = -(\partial F/\partial T)$ is given by

$$S_{el}(T,h^{ext}) = R\left[\sum_{\sigma}\int_{a_\sigma}^{b_\sigma}\ln(1+e^{-\beta(\varepsilon-\mu)})\rho_\sigma(\varepsilon)d\varepsilon + \frac{1}{kT}\sum_{\sigma}\int_{a_\sigma}^{b_\sigma}(\varepsilon-\mu)\rho_\sigma(\varepsilon)f(\varepsilon)d\varepsilon\right]. \quad (12)$$

The lattice entropy S_{lat} in the Debye approximation is given by

$$S_{lat}(T) = \left\{-3R\ln\left[1-\exp\left(\frac{\Theta_D}{T}\right)\right] + 12R\left(\frac{T}{\Theta_D}\right)^3\int_0^{\Theta_D/T}\frac{x^3}{\exp(x)-1}dx\right\}, \quad (13)$$

where Θ_D is the Debye temperature. Hence the total entropy of the intermetallic compounds is given by

$$S(T,h^{ext}) = S_{lat}(T) + S_{mag}(T,h^{ext}), \quad (14)$$

where the magnetic entropy S_{mag} is given by

$$S_{mag}(T,h^{ext}) = S_{loc}(T,h^{ext}) + S_{el}(T,h^{ext}). \quad (15)$$

III. NUMERICAL RESULTS AND DISCUSSION

In order to apply the model described in the preceding section to calculate the magnetocaloric effect in the $R\mathrm{Co}_2$ series (R=Dy, Ho, Er), we have to specify a set of model parameters. The total angular momentum J^f and the g factors were extracted from Hund's rule. The exchange interaction parameters J_{df} and J_0 were properly chosen to describe the experimental value of the magnetic ordering temperature of each intermetallic compound of the series. The paramagnetic $3d$ density of states was taken from first-principles calculations.[34] The factor U parametrizing the Coulomb interaction between itinerant electron was chosen to assure that the Stoner criterion for the magnetic order at the Co site is not fulfilled, despite that one has a strongly enhanced Pauli paramagnetism. All these parameters are kept fixed during the entire self-consistent process. In order to carry out the self-consistent process, we start with an initial value of $\langle J^f\rangle$ and calculate the electronic magnetic moment $\langle m^d\rangle$ of the subsystem of the itinerant electrons. After that, using the equations for the subsystem of localized spins to calculate a new value of $\langle J^f\rangle$. Then we return to the subsystem of the itinerant electrons to calculate a new value of the magnetic moment $\langle m^d\rangle$. We repeat this process until self-consistent values of $\langle J^f\rangle$ and $\langle m^d\rangle$ are obtained within the desired numerical precision.

First, we discuss the case of the intermetallic compound ErCo_2. In this compound, a magnetic moment of 1.0 μ_B at Co site is induced in an antiparallel way to the Er one. The total magnetization curve exhibits a first-order magnetic phase transition at T_c=33 K, and the easy magnetization direction[25] is $\langle 111\rangle$. The crystal-field parameters for this intermetallic compound were taken as:[27] $x=-0.24$; $W=-0.49$ K, $F_4=60$, and $F_6=13\,860$. After determining self-consistently the energy eigenvalues and the spin-polarized density of states, we calculate the contributions to the total entropy without an applied magnetic field. In the calculation of the lattice contribution we take the Debye temperature as $\Theta_D=240$ K.[35] The dotted line of Fig. 1 shows our calculated total entropy of the ErCo_2 intermetallic compound at zero magnetic field. The jump observed in this curve, around the magnetic ordering temperature, is due to the magnetic part of the entropy. Moreover, it turns out that the contribution of the itinerant electrons to the magnetic entropy is very small as compared to the contribution from the localized spins. Actually, the magnetic part of the entropy saturates around $R\ln(2J+1)$, which is the expected saturation value of the magnetic entropy for the $4f$ localized spins. However, the jump in the magnetic part of the entropy is due to the coupling between the $3d$ itinerant electrons and the $4f$ localized spins.

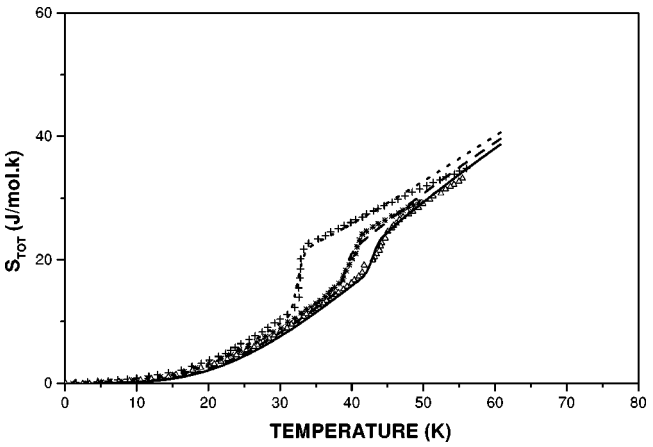

FIG. 1. Temperature dependence of the total entropy in the ErCo_2 intermetallic compound. The dotted, dashed and solid lines correspond to our calculations for a applied magnetic field of 0 T, 4 T, and 6 T, respectively. Crosses, stars, and triangles represent experimental data.[25]

In order to calculate the magnetic entropy change for a given magnetic-field variation, we apply the magnetic field along the easy magnetization direction. The dashed and solid lines of Fig. 1 represent the total entropy for an external magnetic field of 4 T and 6 T, respectively. Notice that we have a good agreement with experimental data[25] for all curves. The curves of the isothermal magnetic entropy change ($\Delta S_{mag}\times T$) and of the adiabatic temperature change ($\Delta T_{ad}\times T$) for a magnetic-field variation from 0–2 T, 0–4 T, and 0–6 T are plotted in Figs. 2 and 3, respectively. From these figures, we can observe that both the isothermal magnetic entropy change and the adiabatic temperature change for the three above-mentioned magnetic-field variation exhibit a jump at around the magnetic ordering temperature, yielding a large value of the magnetocaloric potential in the ErCo_2 intermetallic compound. This is directly associated with the first-order magnetic phase transition that is due to the coupling between the itinerant electrons and the localized spins.

Second, we perform numerical calculations for the intermetallic compound HoCo_2. This compound exhibits a first-

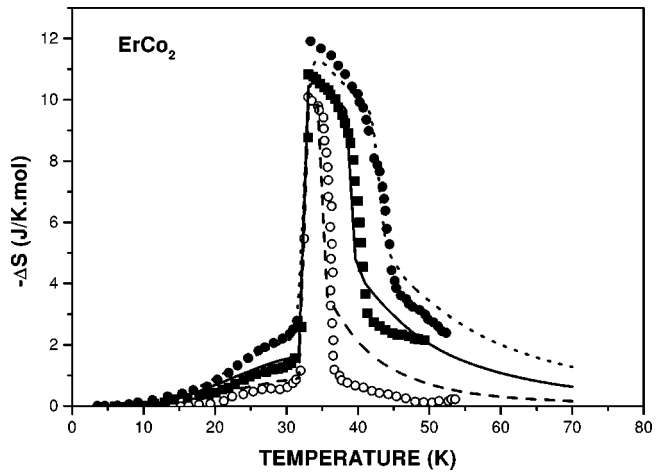

FIG. 2. Isothermal magnetic entropy change vs T in the compound $ErCo_2$. The dashed, solid and dotted lines correspond to our calculations for a magnetic-field variation 0–2 T, 0–4 T, and 0–6 T, respectively. Open circles, squares, and full circles represent experimental data.[25]

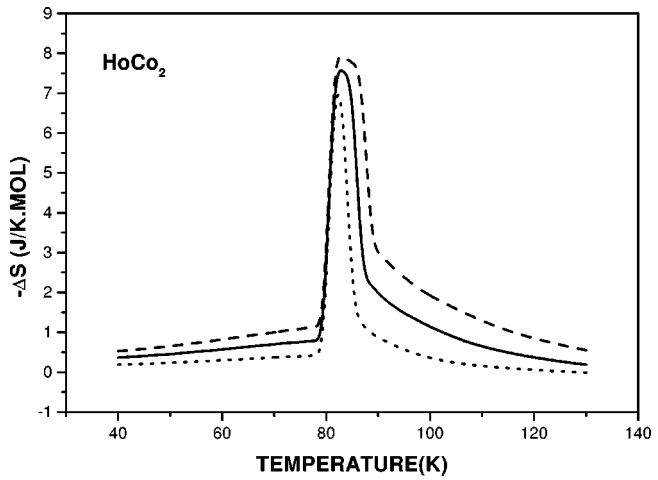

FIG. 4. Isothermal magnetic entropy change vs T in the compound $HoCo_2$. The dotted, solid, and dashed lines correspond to our calculations for a magnetic-field variation 0–2 T, 0–4 T, and 0–6 T, respectively .

order magnetic phase transition around 80 K and its easy magnetization direction[36]is $\langle 100 \rangle$ above 14 K. As we did before, the Coulomb interaction parameter U was taken to give a strongly enhanced paramagnetic susceptibility near the fulfillment of the Stoner criterion for the onset of a magnetic order at the Co sites. The exchange interaction parameters (J_0, J_{df}) were chosen to adjust the experimental value of the magnetic ordering temperature. In our model, the magnetic ordering temperature and the nature of the magnetic phase transition is determined by the ratio J_0/J_{df}. The first-order magnetic phase transition occurs when the ratio J_0/J_{df} is less than a given critical value. The crystal-field parameters[36] were taken as $x=-0.4687$, $W=0.6$ K, $F_4=60$, and $F_6=13\,860$. In the calculation of the lattice entropy we take the Debye temperature[35] as $\Theta_D=160$ K. In Figs. 4 and 5 we plot, respectively the curves of the isothermal magnetic entropy and of the adiabatic temperature in the $HoCo_2$ intermetallic compound, for a magnetic-field variation 0–2 T (dotted line), 0–4 T (full line), and 0–6 T (dashed line). Notice that we also get a good agreement with the available experimental data[29] for the adiabatic temperature change.

Finally, we perform numerical calculations for the intermetallic compound $DyCo_2$. This compound exhibits a first-order magnetic phase transition at around 130 K. The model parameters for this intermetallic were chosen in a way similar to the previous cases. The behavior of the total entropy in this compound is very similar to those obtained before for the $ErCo_2$ and $HoCo_2$ intermetallic compounds. In Figs. 6 and 7 we show the curves of the isothermal magnetic entropy change $(\Delta S_{mag} \times T)$ and of the adiabatic temperature change $(\Delta T_{ad} \times T)$ in the $DyCo_2$ intermetallic compound for a magnetic-field variation 0–6 T. For the sake of comparison,

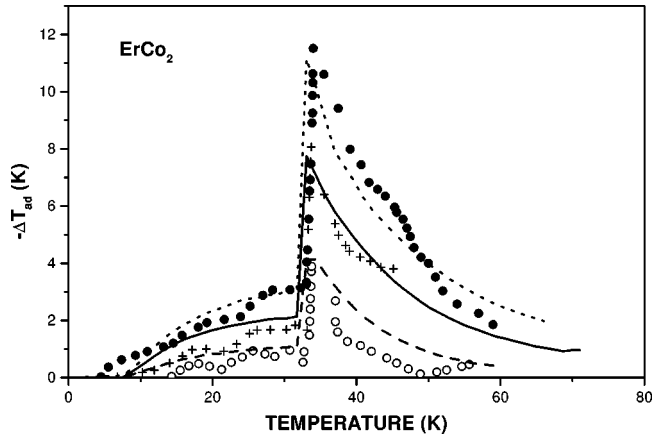

FIG. 3. Adiabatic temperature change vs T in the compound $ErCo_2$. The dashed, solid, and dotted lines correspond to our calculation for a magnetic-field variation 0–2 T, 0–4 T, and 0–6 T, respectively. Open circles, crosses, and full circles represent experimental data.[25]

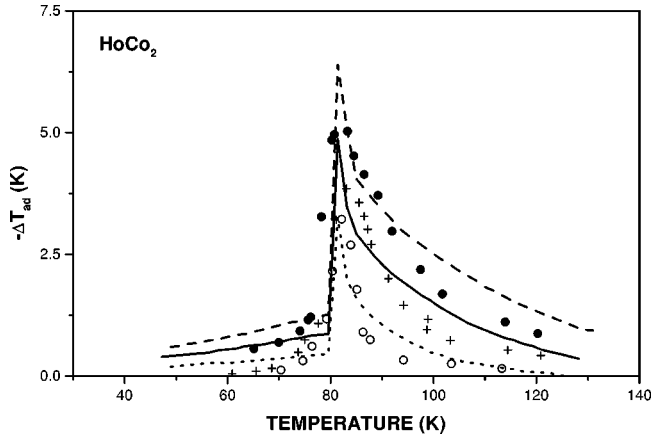

FIG. 5. Adiabatic temperature change vs T in the compound $HoCo_2$. The dotted, solid and dashed lines correspond to our calculations for a magnetic-field variation 0–2 T, 0–4 T, and 0–6 T, respectively. Open circles, crosses, and full circles represent experimental data.[29]

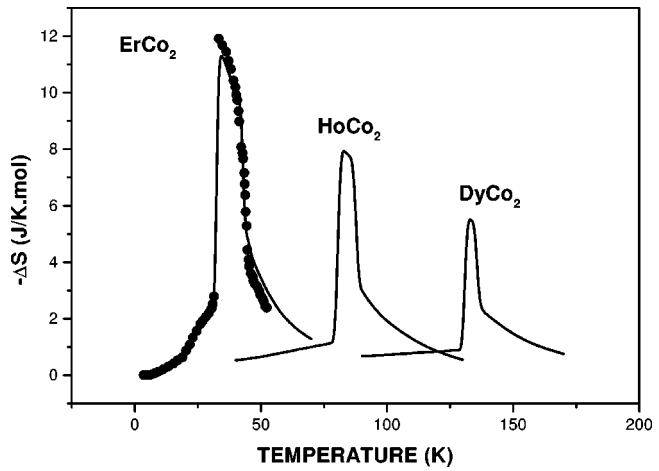

FIG. 6. Isothermal magnetic entropy change vs T in the compounds $ErCo_2$, $HoCo_2$, and $DyCo_2$. The solid lines correspond to our calculations for a magnetic-field variation 0–6 T. Circles are experimental data[25] for $ErCo_2$.

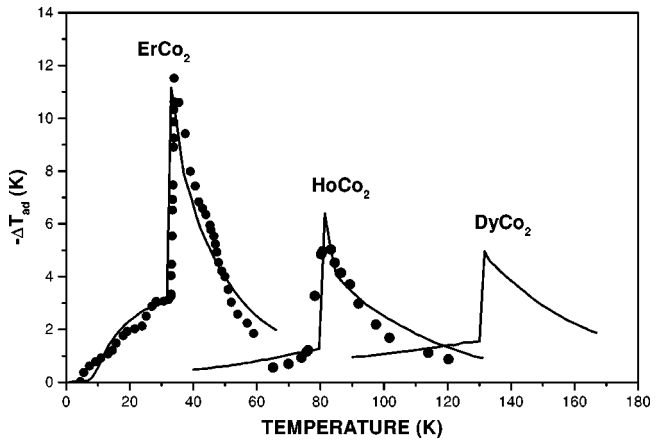

FIG. 7. Adiabatic temperature change vs T in the compounds $ErCo_2$, $HoCo_2$, and $DyCo_2$. The solid lines correspond to our calculation for a magnetic-field variation from 0–6 T. Circles and squares are experimental data,[25,29] for $ErCo_2$ and $HoCo_2$, respectively.

we also plot in these figures the corresponding curves for $ErCo_2$ and $HoCo_2$. From these figures we can observe that the maximum values of ΔS_{mag} and ΔT_{ad} increase with decreasing T_c. This fact can be explained as follows: As the magnetic entropy tends to saturate around the magnetic ordering temperature and as the saturation magnetizations of these three intermetallic compounds are very close, we expect that the smaller the magnetic ordering temperature, the faster the saturation value of the magnetic entropy is reached. Accordingly, the maximum values in the magnetocaloric potentials ΔS_{mag} and ΔT_{ad} decrease as we go from $ErCo_2$ ($T_c = 33$ K) to $DyCo_2$ ($T_c = 130$ K), as it is experimentally observed.

In conclusion, in this paper we have calculated the magnetocaloric effect in the series RCo_2(R=Er, Dy, Ho). In the magnetocaloric curves of these intermetallic compounds, an abrupt enhancement is observed around the magnetic ordering temperature. It is worthwhile to point out here that although the main contribution to the magnetic entropy in the RCo_2 intermetallic compounds comes from the localized spins, the jump observed in the magnetic entropy curve around the magnetic ordering temperature is due to the coupling between the localized spins of the rare-earth ions and the magnetic moment induced at the Co sites. We can straightforwardly extend the model presented in this paper to study the effect of an external pressure and doping on the magnetocaloric properties of the rare-earth transition-metal intermetallics. In addition, the case of RFe_2, where it is expected a major contribution from the $3d$ itinerant electrons of the Fe ions, can be also described using the model discussed throughout this paper. Calculations in these directions are now in progress.

ACKNOWLEDGMENTS

We would like to thank Conselho Nacional de Desenvolvimento Científico e Tecnológico-CNPq/Brazil and Fundação de Amparo a Pesquisa do Estado do Rio de Janeiro-FAPERJ/Brazil for partial financial support. This work was partially performed under the frame of PRONEX—Project No. 66201998-9.

[1] V.K. Pecharsky and K.A. Gschneidner, Jr., J. Magn. Magn. Mater. **200**, 44 (1999), and reference cited therein.

[2] V.K. Pecharsky and K.A. Gschneidner, Jr., Phys. Rev. Lett. **78**, 4494 (1997).

[3] V.K. Pecharsky and K.A. Gschneidner, Jr., J. Magn. Magn. Mater. **167**, L179 (1997).

[4] V.K. Pecharsky and K.A. Gschneidner, Jr., J. Alloys Compd. **260**, 98 (1997).

[5] V.K. Pecharsky and K.A. Gschneidner, Jr., Appl. Phys. Lett. **70**, 3299 (1997).

[6] V.K. Pecharsky and K.A. Gschneidner, Jr., Adv. Cryog. Eng. **43**, 1729 (1998).

[7] X. Bohigas, J. Tejada, E. del Barco, X.X. Zhangg, and M. Sales, Appl. Phys. Lett. **73**, 390 (1998).

[8] Young Sun, Xiaojun Xu, and Yuheng Zhang, J. Magn. Magn. Mater. **219**, 183 (2000).

[9] Z.M. Wang, G. Ni, Q.Y. Xu, H. Sang, and Y.W. Du, J. Magn. Magn. Mater. **234**, 371 (2001).

[10] F. Torres, J.M. Hernandez, X. Bohigas, and J. Tejada, Appl. Phys. Lett. **77**, 3248 (2000).

[11] R.D. Schull and L.H. Bennet, J. Nanostructured Materials **1**, 83 (1992).

[12] B.J. Korte, V.K. Pecharsky, and K.A. Gschneidner, Jr., J. Appl. Phys. **84**, 5677 (1998).

[13] P.J. von Ranke, V.K. Pecharsky, K.A. Gschneidner, Jr., and B.J. Korte Phys. Rev. B **58**, 12110 (1998).

[14] P.J. von Ranke, V.K. Pecharsky, and K.A. Gschneidner, Jr., Phys. Rev. B **58**, 14436 (1998).

[15] P.J. von Ranke, I.G. de Oliveira, A.P. Guimarães, and X. A da Silva, Phys. Rev. B **61**, 447 (2000).
[16] I.G. de Oliveira, A. Caldas, E.P. Nóbrega, N. A de Oliveira, and P.J. von Ranke Solid State Commun. **114**, 487 (2000).
[17] P.J. von Ranke, N. A de Oliveira, M.V. Tovar Costa, E.P. Nóbrega, A. Caldas, and I.G. de Oliveira, J. Magn. Magn. Mater. **226-230**, 970 (2001).
[18] A.C. Hewson, *The Kondo Problem to Heavy Fermions* (Cambridge University press, Cambridge, UK, 1993), p. 109.
[19] P.J. von Ranke, N.A. de Oliveira, M.V. Tovar Costa, and A. Troper, J. Appl. Phys. **91**, 8879 (2002).
[20] P.J. von Ranke, A.L. Lima, E.P. Nóbrega, X. A da Silva, A.P. Guimarães, and I.S. de Oliveira, Phys. Rev. B **63**, 024422 (2001).
[21] P.J. von Ranke, E.P. Nóbrega, I.G. de Oliveira, A.M. Gomes, and R.S. Sarthour, Phys. Rev. B **63**, 184406 (2001).
[22] T. Hashimoto, K. Matsumoto, T. Kurihara, T. Numuzawa, A. Tomokiyo, H. Yayama, T. Goto, S. Todo, and M. Sahashi, Adv. Cryog. Eng. **32**, 279 (1986).
[23] T. Hashimoto, T. Kuzuhara, K. Matsumoto, M. Sahashi, K. Inomata, A. Tomokiyo, and H. Yayama, Jpn. J. Appl. Phys., Part 1 **26**, 1673 (1987).
[24] T. Hashimoto, T.T. Kuzuhara, M. Sahashi, K. Inomata, A. Tomokiyo, and H. Yayama, J. Appl. Phys. **62**, 3873 (1987).
[25] H. Wada, S. Tomekawa, and M. Shiga, Cryogenics **39**, 915 (1999).
[26] H. Wada, S. Tomekawa, and M. Shiga, J. Magn. Magn. Mater. **196-197**, 689 (1999).
[27] H. Imai, H. Wada, and M. Shiga, J. Magn. Magn. Mater. **140-144**, 835 (1995).
[28] P.J. von Ranke, E. P. Nóbrega, I.G. de Oliveira, A.M. Gomes, and R.S. Sarthour J. Alloys Compd. (to be published).
[29] S.A. Niktin and A.M. Tishin Cryogenics **31**, 166 (1991).
[30] O. Tegus, E. Brück, K.H.J. Buschow, and F.R. de Boer, Nature (London) **415**, 150 (2002).
[31] M. Sakoh and D.M. Edwards Phys. Status Solidi B **70**, 611 (1975).
[32] K.R. Lea, M.J. Leask, and W.P.J. Wolf, J. Phys. Chem. Solids **23**, 1381 (1962).
[33] M.T. Hutchings Solid State Phys. **16**, 227 (1964).
[34] O. Syshchenko, T. Fujita, V. Sechovsky, M. Divis, and H. Fujii, J. Magn. Magn. Mater. **226-230**, 1062 (2001).
[35] N. Pillmayr, G. Hilscher, E. Gratz, and V. Sechovsky, J. Phys. C **8**, 273 (1988).
[36] D. Gignoux, F. Givord, and R. Lemaire, Phys. Rev. B **12**, 3878 (1975).